



OPEN ACCESS

EDITED BY

Jianhui Tang,
Chinese Academy of Sciences (CAS), China

REVIEWED BY

Dasa Gu,
Hong Kong University of Science and
Technology, Hong Kong SAR, China
Jianhui Ye,
Southern University of Science and Technology,
China

*CORRESPONDENCE

Yanli Zhang,
✉ zhang_yl86@igig.ac.cn

RECEIVED 04 September 2024

ACCEPTED 23 September 2024

PUBLISHED 02 October 2024

CITATION

Pang W, Zhang Y, Zeng J, Tian X and Wang X
(2024) Modulating effects of temperature on
CO₂-inhibited isoprene emissions in
Eucalyptus urophylla.
Front. Environ. Sci. 12:1490552.
doi: 10.3389/fenvs.2024.1490552

COPYRIGHT

© 2024 Pang, Zhang, Zeng, Tian and Wang. This
is an open-access article distributed under the
terms of the [Creative Commons Attribution
License \(CC BY\)](#). The use, distribution or
reproduction in other forums is permitted,
provided the original author(s) and the
copyright owner(s) are credited and that the
original publication in this journal is cited, in
accordance with accepted academic practice.
No use, distribution or reproduction is
permitted which does not comply with these
terms.

Modulating effects of temperature on CO₂-inhibited isoprene emissions in *Eucalyptus urophylla*

Weihua Pang^{1,2}, Yanli Zhang^{1,2*}, Jianqiang Zeng¹, Xiao Tian¹ and Xinming Wang^{1,2}

¹State Key Laboratory of Organic Geochemistry and Guangdong Key Laboratory of Environmental Protection and Resources Utilization, Guangzhou Institute of Geochemistry, Chinese Academy of Sciences, Guangzhou, China, ²College of Resources and Environment, University of Chinese Academy of Sciences, Beijing, China

Terrestrial vegetation emits substantial amounts of highly reactive isoprene, significantly impacting atmospheric chemistry and climate change. Both atmospheric carbon dioxide (CO₂) concentration and temperature can influence plant isoprene emissions; however, whether these factors have a synergistic effect remains unclear, particularly for tropical/subtropical plants. In this study, we conducted *in-situ* controlled experiments on *Eucalyptus urophylla*, a representative tropical/subtropical species, to investigate the seasonal variation in the response of isoprene emissions to CO₂ concentrations (ISOP-CO₂ response) and to identify potential controlling factors. The results showed that high CO₂ exerts a nearly linear inhibitory effect on isoprene emissions, as indicated by the slope of the ISOP-CO₂ response curve. This inhibitory effect exhibited evident seasonal changes, with stronger suppression during cooler seasons and weaker suppression during warmer seasons. This finding contrasts with the default ISOP-CO₂ response in the MEGAN model, which ignored seasonal variation. Further analysis showed a significant correlation between the slope of the ISOP-CO₂ response curve and growth temperature from the past 10 days, indicating that these metrics are effective indicators for predicting seasonal changes. Our findings reveal a synergistic mechanism between temperature and CO₂ concentration effects on isoprene emissions. By coupling the effects of growth temperature with the ISOP-CO₂ response, this mechanism can be integrated into models to provide more accurate predictions of future isoprene emissions, reducing prediction biases, especially during cooler seasons.

KEYWORDS

biogenic volatile organic compounds (bvocs), isoprene, tropical/subtropical, isoprene-CO₂ response, *Eucalyptus urophylla*

1 Introduction

The global total emissions of biogenic volatile organic compounds (BVOCs) from terrestrial vegetation exceed 1 Pg yr⁻¹, which is nearly ten times the amount of anthropogenic VOC emissions (Guenther et al., 1995), with isoprene accounting for nearly half of total BVOC emissions (Guenther et al., 2012; Sindelarova et al., 2014; Messina et al., 2016). Due to its huge emissions and high reactivity, isoprene plays a crucial

role in influencing the atmospheric hydroxyl radical budget and contributes significantly to the formation of regional ozone (O₃) and secondary organic aerosols (Pierce et al., 1998; Claeys et al., 2004; Mentel et al., 2013; Harper and Unger, 2018), further impacting global climate (Goldstein et al., 2009; Ehn et al., 2014). Thus, accurate estimation of isoprene emissions is essential for assessing its impact on atmospheric chemical processes and climate change.

Isoprene emissions are influenced by several environmental factors, including temperature, light, and CO₂ concentration (Loreto and Schnitzler, 2010; Peñuelas and Staudt, 2010; Monson et al., 2013; Lantz et al., 2019a; Sharkey et al., 2020). Numerous studies have extensively explored the effects of temperature and light on isoprene emissions, leading to the development of the light-temperature emission mechanism, which is widely used to estimate isoprene emissions at both regional and global scales (Monson and Fall, 1989; Loreto and Sharkey, 1990; Guenther et al., 1995; 2006; 2012; Monson et al., 2007; Mutanda et al., 2016; Higa et al., 2018; Sharkey et al., 2020). In contrast, research on the impact of CO₂ on isoprene emissions is relatively sparse, despite a general consensus that high CO₂ concentrations inhibit isoprene emissions (Wilkinson et al., 2009; Possell and Hewitt, 2011; Lantz et al., 2019b; Yang et al., 2021). However, the mechanism behind this inhibition is not fully understood and remains at the hypothesis stage (Rosenstiel et al., 2003; Rasulov et al., 2009; 2018; Lantz et al., 2019b).

Despite the uncertainties, previous studies have developed an algorithmic relationship between isoprene emissions and CO₂ concentrations based on limited experimental data from temperate plants (Possell et al., 2005; Heald et al., 2009; Wilkinson et al., 2009; Sun et al., 2012), and this algorithm has been incorporated into widely used models such as the Model of Emissions of Gases and Aerosols from Nature (MEGAN) (Guenther et al., 2012). However, the ISOP-CO₂ response relationship varies significantly among different plant species, as shown by the inconsistent suppression of isoprene emissions under high CO₂ concentrations (Lantz et al., 2019b; Niinemets et al., 2021). This suggests that using constant algorithm parameters in global isoprene emission models may introduce significant uncertainties. Relative to temperate plants, numerous studies have demonstrated differences in the light-temperature mechanism of isoprene emission in tropical plants (Kuhn et al., 2004; Guenther et al., 2006; Bracho-Nunez et al., 2013; Higa et al., 2018; Mu et al., 2022; Zeng et al., 2023). However, there is a significant lack of understanding of the ISOP-CO₂ response in tropical plants. It remains unclear whether the CO₂ response mechanism in tropical species differs from that of temperate species and whether modeling algorithms based on temperate plants are applicable to tropical plants. Further research is necessary to verify these relationships.

Numerous studies have demonstrated not only species-specific differences but also seasonal variations in the ISOP-CO₂ response (Loreto and Sharkey, 1990; Affek and Yakir, 2002; Monson et al., 2016; Niinemets et al., 2021). Typically, the suppression of isoprene emissions by high CO₂ concentrations is weaker during warmer seasons and stronger during cooler seasons (Monson et al., 2016). Laboratory studies have further found that elevated temperatures can partially counteract the inhibitory effect of high CO₂ concentrations on isoprene emissions (Potosnak et al., 2014; Lantz et al., 2019b; Sahu et al., 2023). These findings suggest that

growth temperature may be the primary driver of the seasonality observed in the ISOP-CO₂ response, and establishing a relationship between ISOP-CO₂ response and growth temperature could effectively account for these seasonal variations. However, in the current MEGAN model, the ISOP-CO₂ response parameters are fixed, and the default response relationship does not adjust for seasonal changes (Wilkinson et al., 2009; Guenther et al., 2012). Therefore, it is essential to incorporate the seasonality of the ISOP-CO₂ response into the model to improve its accuracy. It is essential to note that tropical and subtropical regions experience higher temperatures and less pronounced annual variations than temperate regions. As a result, it remains unclear whether tropical plants exhibit any seasonality in their ISOP-CO₂ response. Further research is needed to accurately reflect the seasonality of the ISOP-CO₂ response in these regions within the model.

Tropical and subtropical regions are major hotspots for isoprene emissions, contributing approximately 80% of global emissions (Guenther et al., 2012). *Eucalyptus urophylla* (*E. urophylla*) is a representative tree species in these regions and is widely distributed across the globe (Wang et al., 2013; Carignato et al., 2020). In South China, *E. urophylla* is a dominant species, comprising over 15% of the forest composition in Guangdong, Guangxi, and Hainan (Zhang and Wang, 2021; Chen et al., 2022; Ouyang et al., 2022). Previous research has identified *E. urophylla* as one of the tree species with the highest potential for isoprene emissions in South China (Zeng et al., 2022a). In light of this, our study conducted an *in-situ* controlled experiment on *E. urophylla* to investigate its ISOP-CO₂ response and the seasonality of this relationship. We also aimed to identify the main factors driving seasonal variations in this response. The findings of this study, which can provide a scientific foundation for understanding the relationship between isoprene emissions and CO₂ response in tropical and subtropical plants and help to improve the ISOP-CO₂ response mechanism in the model, will inspire and motivate future research in this field.

2 Material and methods

2.1 Field measurements

The field measurement site is located in Heshan, Guangdong Province, southern China, near the Heshan National Field Research Station (Heshan-NFRS) of Forest Ecosystems (22.683°N, 112.900°E). The *E. urophylla* forests selected for this study covered an area of more than 25 hm², and were planted and completely natural growth. All individuals in the forests were similar in overall growth, with an age of about 2 years and an average height of about 12–15 m. *In-situ* measurements were carried out in September 2022 (Sep. 2022), March 2023 (Mar. 2023), and October 2023 (Oct. 2023), and more detailed information on sampling sites can be found in the previous study (Zeng et al., 2024).

The CO₂ response curves for isoprene emissions from *E. urophylla* were measured using a portable photosynthesis system (LI-6800, Li-Cor Biosciences, Lincoln, NE, United States). Three trees were randomly selected for each experiment, and one healthy, sunlit and mature leaf per tree was randomly selected for the control experiments, all leaves being 2–2.5 m above the ground. The CO₂

concentration gradients were set at 50, 100, 200, 300, 400, 500, 600, 800, 1,000 ppm, with other environmental factors such as temperature, light (Photosynthetic active radiation, PAR), and relative humidity carefully maintained at 30°C, 1,000 $\mu\text{mol m}^{-2} \text{s}^{-1}$, and 55%, respectively. We used a standard leaf chamber with an area of 6 cm^2 and the circulating air inlet flow rate was set at 500 $\mu\text{mol s}^{-1}$ (~735 mL min^{-1}). The recycle gas passed through an active charcoal VOCs-scrubber and $\text{Na}_2\text{S}_2\text{O}_3$ (Sodium thiosulfate) column to remove BVOCs and O_3 before entering the instrument. The gas from the leaf chamber was divided into two paths, one of which (flow rate is 200 $\mu\text{mol m}^{-2}\text{s}^{-1}$) passed through an infrared gas analyzer (IRGA), and the other (flow rate is 300 $\mu\text{mol m}^{-2}\text{s}^{-1}$) flowed out of the sampling port, and thus could be sampled from the outlet of the chamber. Sampling was initiated 5 min after leaf photosynthesis had fully stabilized, and BVOCs samples were collected using an adsorbent cartridge bedded with Tenax TA and Carbograph 5TD (C2-AAXX-5149, Marks International Ltd., United Kingdom) combined with a portable dual-channel sampler (ZC-QL, Zhejiang Hengda Instrumentation Ltd., China). The sampling flow rate is 200 mL min^{-1} with duration of 5 min, resulting in a sampling volume of 1 L. The collected adsorbent cartridge samples were meticulously stored and analyzed within 1 week, ensuring the thoroughness of our data collection process.

2.2 BVOC laboratory analysis

Adsorbent cartridge samples were analyzed using an automated thermal desorption-gas chromatography/mass spectrometry system (TD-GC/MS, Markes TD-100/Agilent 5975/Agilent 7890). The TD-100 thermally desorbed the adsorbent tubes at 280°C for 10 min, and then the desorbed analytes were transferred by high-purity helium through a transfer line at 180°C to a cryogenic cold trap at -10°C (U-T11PGC-2S, Markes International Ltd., United Kingdom). The cold trap was then rapidly heated to 320°C, and the high-temperature desorbed analytes were carried by helium at a flow rate of 1 mL min^{-1} into an HP-5MS capillary column (30 $\text{m} \times 0.25 \text{ mm} \times 0.25 \mu\text{m}$, Agilent Technologies, Inc., CA, United States) for separation and then analyzed by mass selective detector (MSD, model 5975, Agilent Technologies, Inc., CA, United States). The initial gas chromatography (GC, model 7890, Agilent Technologies, Inc., CA, United States) oven temperature was 35°C (3 min hold), then increased to 100°C at 5°C min^{-1} and hold for 1 min, then to 120°C at 10°C min^{-1} and hold for 12 min, and then to 260°C at 20°C min^{-1} with a final hold for 2 min. The MSD was operated in both scan mode with electron impacting ionization at 70 eV. Target compounds were identified by their retention times and mass spectra and quantified with the standard calibration curves. More details on the identification and quantification methods were described in the previous articles of our group (Zeng et al., 2022a; 2022b; 2024).

2.3 Calculation of emission rates and activity factors

The isoprene emission rate (E , $\text{nmol m}^{-2} \text{s}^{-1}$) can be calculated as (Equation 1):

$$E = \frac{F(C_{out} - C_{in}) \cdot 10^{-6}}{S \cdot 10^{-4}} \quad (1)$$

Where F ($\mu\text{mol s}^{-1}$) is the flow rate of circulating air, here $F = 500 \mu\text{mol s}^{-1}$; C_{out} (nmol mol^{-1}) and C_{in} (nmol mol^{-1}) are the isoprene volume mixing ratio at the outlet and inlet air, respectively; S (cm^2) is the area of the leaf chamber, which was 6 cm^2 ; 10^{-6} is the conversion factor from μmol to mol ; 10^{-4} is the conversion factor from cm^2 to m^2 .

In order to fit the ISOP- CO_2 response curves using the model algorithm, the emission rates measured at different concentration conditions need to be normalized to 400 ppm measurements (Equation 2), respectively, to obtain normalized isoprene- CO_2 response curves:

$$\gamma = \frac{E_{\text{CO}_2}}{E_{400}} \quad (2)$$

Where E_{CO_2} is the actual emission rate at different CO_2 concentrations and E_{400} is the actual emission rate at 400 ppm CO_2 concentration; γ is the activity factor. The normalized response curves were fitted using the CO_2 response algorithm (Equation 3) in MEGAN v2.1:

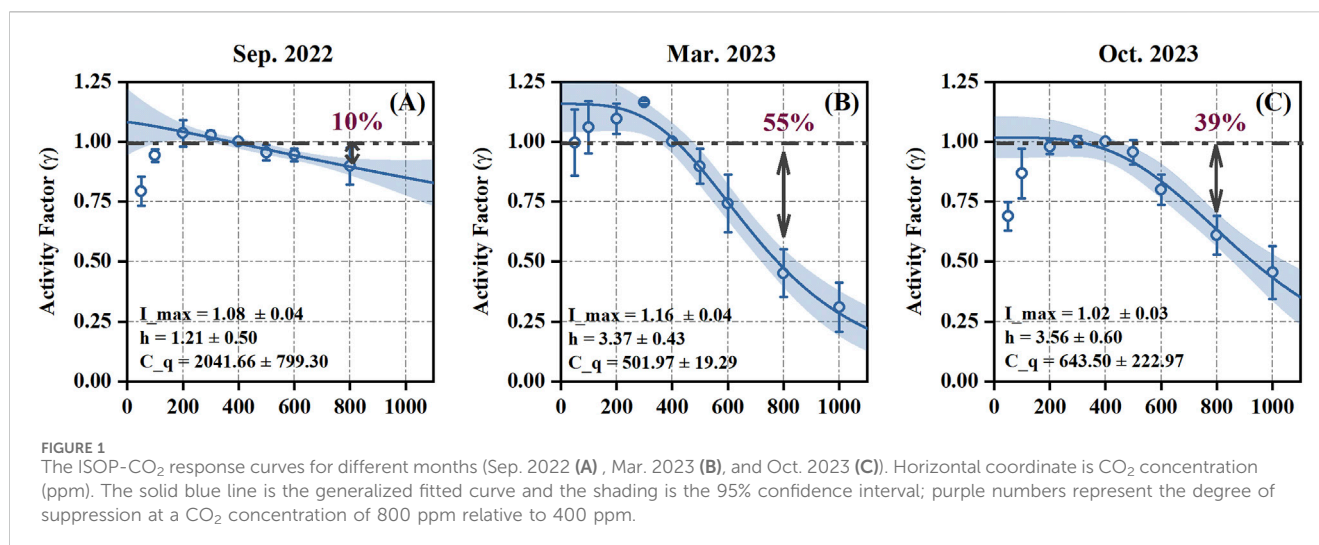
$$\gamma_{c,i} = I_{s,max} \cdot \left[\frac{I_{s,max} \times (0.7C_a)^h}{(C_a)^h + (0.7C_a)^h} \right] \quad (3)$$

Where $I_{s,max}$ is the maximum standardized isoprene emission rate predicted by the algorithm and is unitless; $\gamma_{c,i}$ is the activity factor of isoprene emission; C_a is the CO_2 concentration (ppm); h and C_q are unitless empirical parameters, and the initial values of the fit are the default values of the MEGAN model, specifically, $I_{s,max} = 1.072$; $h = 1.7$; $C^q = 1,218$ (Wilkinson et al., 2009).

3 Results and discussion

3.1 Seasonal changes of ISOP- CO_2 response

The ISOP- CO_2 response curves for *E. urophylla* were obtained through *in situ* control experiments on subtropical Eucalyptus across different seasons. Figure 1 shows the ISOP- CO_2 response curves for three different months, along with the parameter fits derived from the data. The variations in these parameters explain the differences in the peak points and subsequent downward trends of the curves. Although the *E. urophylla* individuals measured each month were randomly selected, the isoprene emission trends in response to CO_2 concentration were consistent among different individuals within the same month. This suggests that the ISOP- CO_2 response pattern is consistent among individuals of the same species during the same month. As illustrated in Figure 1, isoprene emissions peaked as CO_2 concentrations increased from 50 ppm to approximately 200–300 ppm and then decreased, indicating that isoprene emissions from tropical/subtropical *E. urophylla* are suppressed by high levels of CO_2 concentration. The similar suppress phenomenon were also observed for temperate plants (Rosenstiel et al., 2003; Heald et al., 2009; Potosnak et al., 2014; Sharkey and Monson, 2014). While this suppression is common among tree species, there are significant differences in the degree of suppression reported in different studies, indicating species-specific



differences in the ISOP-CO₂ response curves (Niinemets et al., 2021).

Although the extent of isoprene emission suppression by high CO₂ concentrations varied significantly between months, the overall pattern of the ISOP-CO₂ response curve remained relatively consistent within each month. The seasonal variations of ISOP-CO₂ responses showed that relatively stronger suppression in cooler seasons and weaker suppression in warmer seasons. Similar seasonal variations were also found from temperate trees (Monson et al., 2016), and the growth temperature were supposed to contribute to the observed seasonal changes in ISOP-CO₂ response (Potosnak et al., 2014; Lantz et al., 2019b; Sahu et al., 2023). Laboratory experiments on poplar have similarly found that elevated temperatures may counteract this inhibitory effect (Potosnak et al., 2014; McClain and Sharkey, 2019; Sahu et al., 2023). Similarly, from our field experiments conducted in Sep. 2022, Mar. 2023, and Oct. 2023, activity factor of isoprene emission (devoted as γ in Figure 1) decreased by 10%, 55%, and 39% on average in Sep. 2022, Mar. 2023, and Oct. 2023, respectively, at 800 ppm CO₂ when compared to the emissions at 400 ppm CO₂, with daytime mean temperatures of 32.1°C, 22.9°C, and 28.7°C, respectively. These findings align with other studies suggesting that growth temperature is a potential factor driving the seasonal changes in the ISOP-CO₂ response and demonstrating a synergistic effect of temperature and CO₂ on isoprene emissions. However, the effects of temperature and CO₂ on isoprene emissions are currently treated as independent modules in the MEGAN model (Guenther et al., 2012). As global temperatures and CO₂ concentrations increase together, incorporating the synergistic effects of temperature and CO₂ into the model will be crucial for accurately simulating and understanding the future impacts of climate change on isoprene emissions.

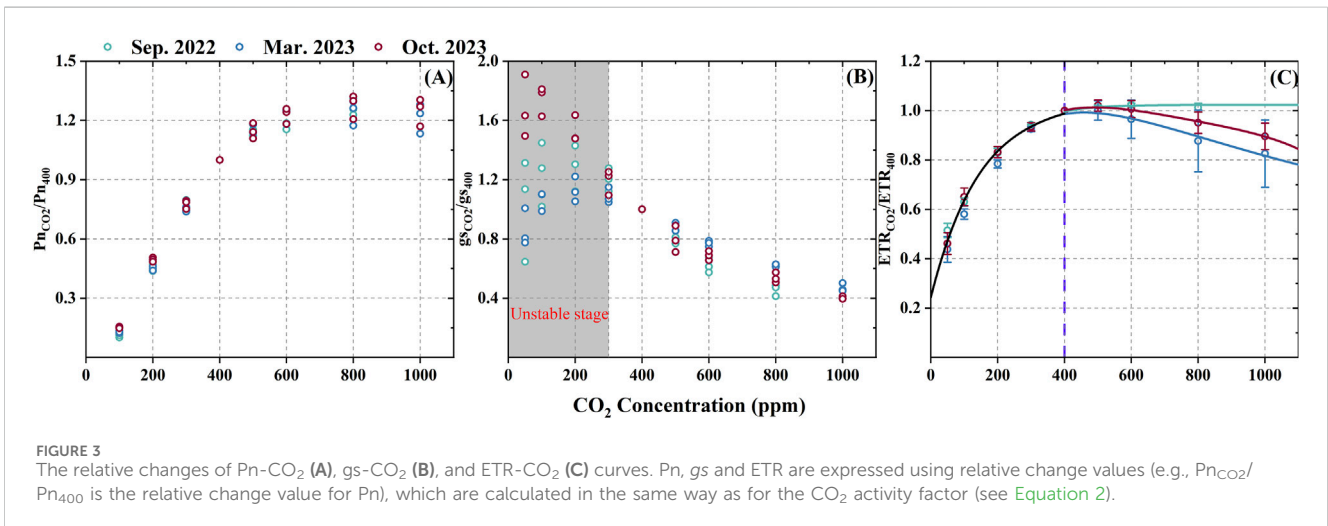
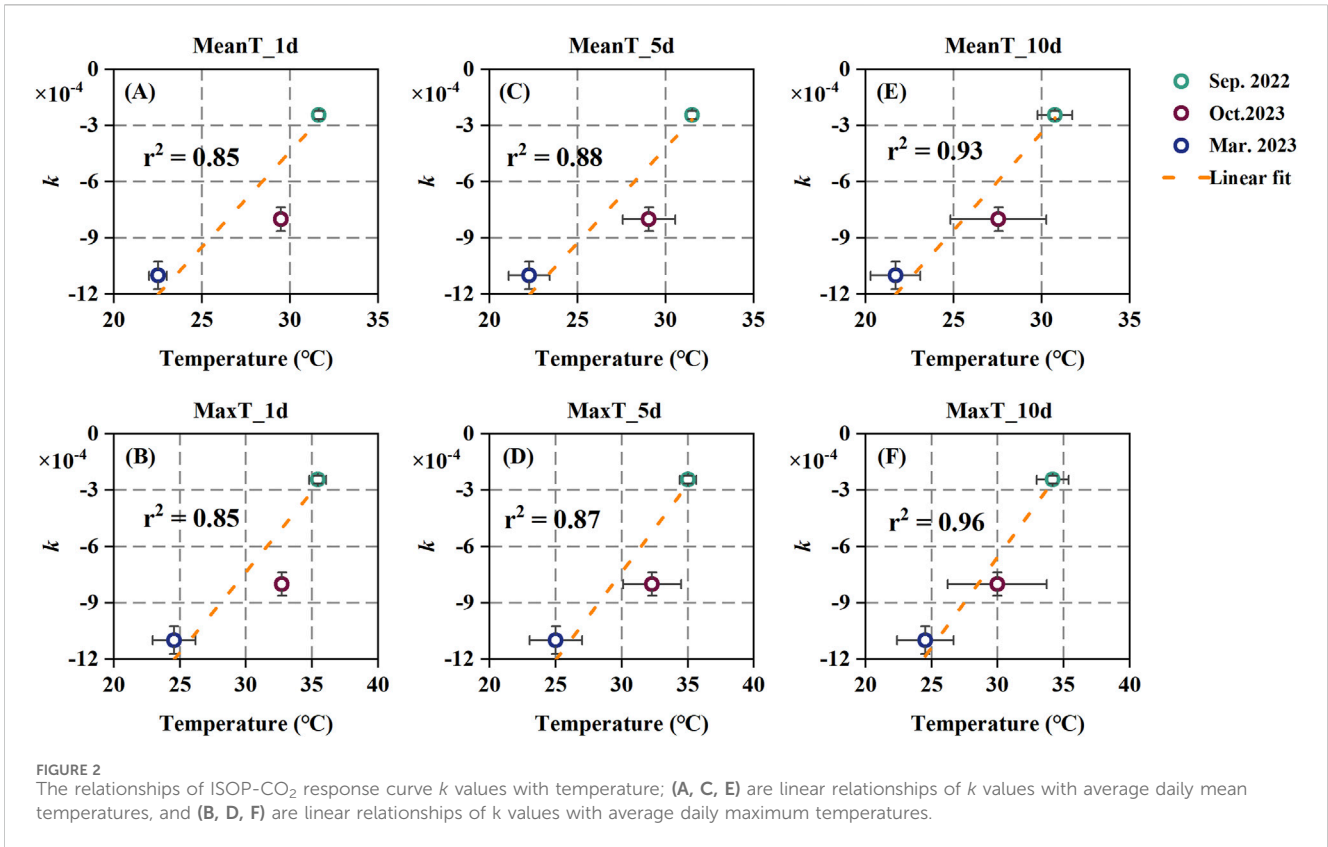
3.2 Factors influencing the seasonal variation of ISOP-CO₂ response

To further investigate the coupling between temperature and ISOP-CO₂ response, we linearly fitted the ISOP-CO₂ response curves within this CO₂ concentration range (e.g.,

400–1,000 ppm), using the slope (k value) to characterize the degree of suppression, and explored the seasonal variations of the k value in relation to different temperature. The study on subtropical Eucalyptus demonstrates that the seasonality of the ISOP-CO₂ response curve is correlated with growth temperature. The linear fitting results revealed that the k values of the ISOP-CO₂ response curves for Sep. 2022, Mar. 2023, and Oct. 2023 were -2.4×10^{-4} , -11.0×10^{-4} , and -8.0×10^{-4} , respectively (Supplementary Figure S1). This correlation may arise from changes in the sensitivity of isoprene emissions to CO₂ as a result of plant adaptation to growth temperature or modifications in isoprene emissions (Niinemets and Sun, 2015; Lantz et al., 2019a; 2019b; Sahu et al., 2023).

Previous studies have shown that isoprene emission factors are influenced by the average temperature over the past 1–10 days, indicating an adaptive mechanism of isoprene emission to growth temperature (Sharkey et al., 1999; Rapparini et al., 2004; Guenther et al., 2012). We selected the average daily mean temperature (TEMP_{mean}) and the average daily maximum temperature (TEMP_{max}) for the past 1-, 5-, and 10-day, respectively, as indicators of growth temperature. The temperature data were obtained from the Heshan National Field Research Station of Forest Ecosystems (<http://hsf.cern.ac.cn/>). As shown in Figure 2, a significant correlation ($p < 0.05$) between the k values and temperature with correlation coefficient (r^2) values ranging from 0.85 to 0.96 were obtained. The overall correlation between the k value and the TEMP_{max} was slightly higher than with the TEMP_{mean}. Additionally, the correlation between k values and the temperature over the past 10-day was generally higher than in the past 5- and 1-day. Moreover, the r^2 values between the k value and the TEMP_{mean} and TEMP_{max} over the past 10-days exceeded 0.90 (0.93 and 0.96, respectively), suggesting that the past 10 days temperature can be used as indicators for predicting the seasonal pattern of the ISOP-CO₂ response.

Besides the environment factors, the variation in plant physiological parameters, such as photosynthesis (Pn), stomatal conductance (g_s), and electron transfer rate (ETR), that could influence the ISOP-CO₂ response curve were also investigated. As shown in Figure 3, these parameters were expressed as



relative changes. The Pn-CO₂ curves for Sep. 2022, Mar. 2023, and Oct. 2023 displayed consistent trends. Photosynthetic activity increased rapidly with CO₂ concentration from a negative value to approximately 1.2 when CO₂ reached 600 ppm, after which it plateaued, indicating a saturation point under high CO₂ conditions (Figure 3A). The *g_s* showed considerable variation at low CO₂ concentrations (<300 ppm), but the *g_s*-CO₂ curves exhibited high consistency as CO₂ concentration increased (Figure 3B). However, the ETR-CO₂ curves followed a similar trend to the Pn-CO₂ curves but with noticeable seasonal changes. Specifically, the ETR-CO₂

curves were consistent across months at lower CO₂ concentrations (<400 ppm), but diverged significantly at higher CO₂ concentrations, stabilizing in the high-temperature month (Sep. 2022) and decreasing in cooler months (Mar. 2023 and Oct. 2023). The ETR-CO₂ curves for Mar. 2023 and Oct. 2023 decreased by 12.4% and 5.0%, respectively, at 800 ppm compared to 400 ppm CO₂ (Figure 3C).

Plant physiological states can be influenced by factors such as PAR, temperature, CO₂ concentration, or biotic stressors (e.g., viruses, pests) (Mu et al., 2022). However, since we chose healthy

and sunlight leaves during our experiments, the effects of factors like PAR, viruses, and pests can be disregarded. The consistent Pn-CO₂ curves across the three experiments suggest that photosynthetic activity remained stable despite seasonal variations (Figure 3), likely due to isoprene synthesis utilizing only 1%–2% of the carbon fixed by photosynthesis (Niinemets et al., 2021). The *g_s* also showed consistent trends at high CO₂ concentrations across months, while variations at low CO₂ concentrations were likely due to unstable stress responses affecting stomatal behavior (Monson et al., 2013; Oikawa and Lerdau, 2013; De Souza et al., 2018). These findings align with other studies showing that *g_s* does not significantly impact isoprene emissions (Sahu et al., 2023), implying that *g_s* is not a major factor in the seasonal variation of ISOP-CO₂ curves.

A prevailing hypothesis suggested that the suppression of the ISOP-CO₂ response curve is due to limitations in the availability of key substances such as adenosine triphosphate (ATP) and nicotinamide adenine dinucleotide phosphate (NADPH) (Niinemets et al., 1999; Rosenstiel et al., 2003; Rasulov et al., 2009; 2016; 2018; Morfopoulos et al., 2014). Based on this, the triose phosphate utilization (TPU) limitation hypothesis was proposed, which posits that under high CO₂ concentrations, the rate of increase in photosynthesis outpaces the rate at which glyceraldehyde 3-phosphate (GAP) is utilized by the methylerythritol 4-phosphate (MEP) pathway. This leads to inorganic phosphate (Pi) accumulation in chloroplasts, which is then incorporated into phosphorus-containing sugars, thereby inhibiting ATP synthesis (McClain and Sharkey, 2019). Although Lantz et al. (2019b) argued that TPU limitation is not essential for suppressing isoprene emissions under high CO₂ concentrations, its presence can still influence the degree of suppression. Furthermore, TPU limitation may be alleviated at higher temperatures, as increased respiration rates and upregulated enzyme activity in the MEP pathway facilitate the release of accumulated Pi, thereby removing the TPU limitation (Monson et al., 2016). Evidence for this was observed in our experimental results, where the ETR-CO₂ curves did not exhibit suppression at high CO₂ concentrations during the warm month (Sep. 2022). In contrast, such suppression was evident in cooler months (March and October 2023) (Figure 3C). The more significant decrease in Mar. 2023 compared to Oct. 2023 is likely attributable to the lower average daytime mean temperatures in March (22.9°C vs. 28.7°C, respectively).

The reduction in the ETR-CO₂ curve at high concentrations is considered characteristic of TPU limitation (McClain and Sharkey, 2019). It can be used to infer whether leaves are experiencing this limitation, which rarely occurs at temperatures above 30°C. This suggests that temperature is likely a key factor controlling the seasonality of the ISOP-CO₂ response, as other major influences did not significantly alter the plant's physiological state. Our study further supports this, showing that this acclimatization mechanism is reflected in the ISOP-CO₂ response curve.

Over time, the correlation between temperature indicators and the *k* value of the ISOP-CO₂ response curve was higher over the past 10 days compared to the past 5 and 1 days, suggesting that this acclimation mechanism has a delayed effect. This delay may be related to physiological adjustments made by plants in response to temperature changes, such as alterations in membrane permeability, the expression of specific functional genes, and the synthesis of

secondary metabolites like isoprenoid compounds (Jagdish et al., 2021; Wang et al., 2024). The slightly higher overall correlation between the *k* value and TEMP_{max} compared to TEMP_{mean} suggests that heat stress may also affect the ISOP-CO₂ response, likely due to the plant's stress response to sudden temperature changes, which could involve regulating isoprene emission, stomatal conductance, and respiration rate (Li and Sharkey, 2013; Li et al., 2020). Given the strong correlation between the *k* value with the TEMP_{mean} and the TEMP_{max} over the past 10 days (with correlation coefficients larger than 0.90), it is possible to model the relationship between temperature and the ISOP-CO₂ response by further incorporating the effects of temperature on the *k* value (Figure 2).

3.3 Implications for current and future isoprene emissions simulations

The comparison of the ISOP-CO₂ response curves for each month with the model default response curves and found that the model (MEGAN default $k = -3.7 \times 10^{-4}$) predicts stronger suppression of isoprene emissions at high CO₂ concentrations than what was observed in Sep. 2022, but weaker suppression compared to Mar. 2023 and Oct. 2023 (Supplementary Figure S2). This leads to an underestimation of isoprene emissions during the high-temperature months and an overestimation during the low-temperature months. For example, at a CO₂ concentration of 800 ppm, the model underestimates emissions by 5% in Sep. 2022 but overestimates the emissions by 38% in Mar. 2023 and 21% in Oct. 2023, respectively. Therefore, to lower the uncertainties of isoprene emission simulation, it is important to account for seasonal variations in the ISOP-CO₂ response, such as by incorporating the effect of the TEMP_{max} over the past 10 days, as suggested above.

Even though the strong suppression of isoprene emissions only occurred under high CO₂ concentrations, not the current state. Under climate change, wildfires' extent, frequency, intensity, and duration have increased recently, leading to significant spikes in atmospheric CO₂ concentrations and regional temperatures in localized areas. For example, during the Australian wildfires of 2019–2020, CO₂ concentrations in smoke-covered regions increased by 5- to 80-fold (Van Der Velde et al., 2021; Hong et al., 2023). Under such conditions, isoprene emissions from vegetation surrounding the wildfire perimeter may be severely suppressed by high CO₂ concentrations. However, the accompanying increase in temperature could mitigate the extent of this suppression. Our results provide insights into assessing the impacts of isoprene emissions from vegetation in wildfire-affected regions, which is essential for accurately estimating the consequences of wildfire disasters.

Moreover, according to the IPCC report, global average CO₂ concentrations are expected to reach 900 ppm or higher by the end of the 21st century, and global average temperatures could rise by 1°C–4.5°C (IPCC, 2018). Under future conditions, the suppression of isoprene emissions by CO₂ will become more pronounced. However, this study shows that this effect must account for seasonal variability. Our results also suggest that rising global temperatures may reduce the suppression effect of CO₂ on isoprene emissions in the future. However, current models do not include the coupling mechanism between temperature and

the ISOP-CO₂ response, which could introduce significant uncertainty into predictions of future isoprene emissions. The current model may exhibit a slight prediction bias (e.g., <10%) during future high-temperature seasons or extreme heatwaves, potentially overestimating emissions during cooler seasons. To more accurately predict future isoprene emissions, it is necessary to incorporate the coupling mechanism between temperature and the ISOP-CO₂ response into the model.

Additionally, many studies have shown that elevated atmospheric CO₂ concentrations fertilize terrestrial vegetation, leading to increased net primary productivity and leaf area index (Piao et al., 2012; Forkel et al., 2016; Chen et al., 2019). This increase may partially offset the suppression of isoprene emissions caused by higher CO₂ levels. Therefore, assessing the impact of elevated CO₂ on future isoprene emissions requires a comprehensive approach that considers multiple factors and coupled mechanisms.

4 Conclusion

In this study, we conducted *in situ* control experiments with subtropical *E. urophylla* trees to investigate the responses of their isoprene emissions on CO₂ concentrations. The results demonstrated significant seasonality in the ISOP-CO₂ response of *Eucalyptus*, with isoprene suppression by high CO₂ concentrations being lower during the high-temperature season and higher during the low-temperature season. We inferred that growth temperature is the primary factor driving this seasonal variation. Additionally, we found a strong correlation ($r^2 > 0.9$) between growth temperature indicators, such as the average daytime mean temperature and the average daytime maximum temperature over the past 10 days with the degree of suppression (k). This suggests that these temperature indicators can predict seasonal changes in the ISOP-CO₂ response. Therefore, incorporating the coupling of growth temperature with the ISOP-CO₂ response into models is essential for more accurately predicting isoprene emissions under future climate scenarios or extreme wildfire conditions. Although the ISOP-CO₂ response curve for *E. urophylla* in tropical and subtropical regions has been studied, research on other common tree species is necessary due to the species-specific differences in ISOP-CO₂ responses. Future studies should focus on a broader range of tree species to understand how various physiological traits influence isoprene emissions under elevated CO₂ conditions, which would aid in developing more comprehensive models for predicting emissions at the ecosystem level. Long-term field experiments in natural forests, exposed to varying environmental conditions and stressors, would also help validate findings from controlled studies, providing more realistic insights into how rising CO₂ levels affect isoprene emissions *in situ*. Additionally, future research should explore how elevated CO₂ interacts with other environmental factors, such as temperature, moisture, and pollutants like ozone and nitrogen oxide, to build a more holistic understanding of isoprene emissions. Incorporating empirical data into ecosystem models that account for interspecies interactions, varying tree densities, and different forest management practices can bridge the gap between individual tree studies and broader ecosystem impacts.

Data availability statement

The raw data supporting the conclusions of this article will be made available by the authors, without undue reservation.

Author contributions

WP: Data curation, Investigation, Methodology, Software, Writing–original draft. YZ: Conceptualization, Data curation, Funding acquisition, Investigation, Methodology, Project administration, Resources, Supervision, Writing–review and editing. JZ: Data curation, Investigation, Methodology, Software, Writing–review and editing. XT: Data curation, Investigation, Methodology, Writing–review and editing. XW: Conceptualization, Funding acquisition, Methodology, Project administration, Supervision, Writing–review and editing.

Funding

The author(s) declare that financial support was received for the research, authorship, and/or publication of this article. This work was supported by the National Natural Science Foundation of China (42321003), Guangdong Foundation for Program of Science and Technology Research (2020B1111360001/2023B0303000007/2023B1212060049), Youth Innovation Promotion Association of the Chinese Academy of Sciences (Y2021096), and Guangzhou Municipal Science and Technology Bureau (202206010057).

Conflict of interest

The authors declare that the research was conducted in the absence of any commercial or financial relationships that could be construed as a potential conflict of interest.

The author(s) declared that they were an editorial board member of *Frontiers*, at the time of submission. This had no impact on the peer review process and the final decision.

Publisher's note

All claims expressed in this article are solely those of the authors and do not necessarily represent those of their affiliated organizations, or those of the publisher, the editors and the reviewers. Any product that may be evaluated in this article, or claim that may be made by its manufacturer, is not guaranteed or endorsed by the publisher.

Supplementary material

The Supplementary Material for this article can be found online at: <https://www.frontiersin.org/articles/10.3389/fenvs.2024.1490552/full#supplementary-material>

References

- Affek, H. P., and Yakir, D. (2002). Protection by isoprene against singlet oxygen in leaves. *Plant Physiol.* 129, 269–277. doi:10.1104/pp.010909
- Bracho-Nunez, A., Knothe, N. M., Welter, S., Staudt, M., Costa, W. R., Liberato, M. A. R., et al. (2013). Leaf level emissions of volatile organic compounds (VOC) from some Amazonian and Mediterranean plants. *Biogeosciences* 10, 5855–5873. doi:10.5194/bg-10-5855-2013
- Carignato, A., Vazquez-Pique, J., Tapias, R., Ruiz, F., and Fernandez, M. (2020). Variability and plasticity in cuticular transpiration and leaf permeability allow differentiation of *Eucalyptus* clones at an early age. *Forests* 11, 9. doi:10.3390/f11010009
- Chen, J. M., Ju, W., Ciais, P., Viovy, N., Liu, R., Liu, Y., et al. (2019). Vegetation structural change since 1981 significantly enhanced the terrestrial carbon sink. *Nat. Commun.* 10, 4259. doi:10.1038/s41467-019-12257-8
- Chen, W., Zou, Y., Dang, Y., and Sakai, T. (2022). Spatial distribution and dynamic change monitoring of *Eucalyptus* plantations in China during 1994–2013. *Trees-Struct. Funct.* 36, 405–414. doi:10.1007/s00468-021-02215-7
- Claeys, M., Graham, B., Vas, G., Wang, W., Vermeylen, R., Pashynska, V., et al. (2004). Formation of secondary organic aerosols through photooxidation of isoprene. *Science* 303, 1173–1176. doi:10.1126/science.1092805
- De Souza, V. F., Niinemets, U., Rasulov, B., Vickers, C. E., Duvoisin Junior, S., Araujo, W. L., et al. (2018). Alternative carbon sources for isoprene emission. *Trends Plant Sci.* 23, 1081–1101. doi:10.1016/j.tplants.2018.09.012
- Ehn, M., Thornton, J. A., Kleist, E., Sipila, M., Junninen, H., Pullinen, I., et al. (2014). A large source of low-volatility secondary organic aerosol. *Nature* 506, 476–479. doi:10.1038/nature13032
- Forkel, M., Carvalhais, N., Roedenbeck, C., Keeling, R., Heimann, M., Thonicke, K., et al. (2016). Enhanced seasonal CO₂ exchange caused by amplified plant productivity in northern ecosystems. *Science* 351, 696–699. doi:10.1126/science.aac4971
- Goldstein, A. H., Koven, C. D., Heald, C. L., and Fung, I. Y. (2009). Biogenic carbon and anthropogenic pollutants combine to form a cooling haze over the southeastern United States. *Proc. Natl. Acad. Sci. U.S.A.* 106, 8835–8840. doi:10.1073/pnas.0904128106
- Guenther, A., Hewitt, C. N., Erickson, D., Fall, R., Geron, C., Graedel, T., et al. (1995). A global model of natural volatile organic compound emissions. *J. Geophys. Res. Atmos.* 100, 8873–8892. doi:10.1029/94jd029250
- Guenther, A., Karl, T., Harley, P., Wiedinmyer, C., Palmer, P. I., and Geron, C. (2006). Estimates of global terrestrial isoprene emissions using MEGAN (model of emissions of gases and aerosols from nature). *Atmos. Chem. Phys.* 6, 3181–3210. doi:10.5194/acp-6-3181-2006
- Guenther, A. B., Jiang, X., Heald, C. L., Sakulyanontvittaya, T., Duhl, T., Emmons, L. K., et al. (2012). The model of emissions of gases and aerosols from nature version 2.1 (MEGAN2.1): an extended and updated framework for modeling biogenic emissions. *Geosci. Model Dev.* 5, 1471–1492. doi:10.5194/gmd-5-1471-2012
- Harper, K. L., and Unger, N. (2018). Global climate forcing driven by altered BVOC fluxes from 1990 to 2010 land cover change in maritime Southeast Asia. *Atmos. Chem. Phys.* 18, 16931–16952. doi:10.5194/acp-18-16931-2018
- Heald, C. L., Wilkinson, M. J., Monson, R. K., Alo, C. A., Wang, G., and Guenther, A. (2009). Response of isoprene emission to ambient CO₂ changes and implications for global budgets. *Glob. Change Biol.* 15, 1127–1140. doi:10.1111/j.1365-2486.2008.01802.x
- Higa, T., Parveen, S., Mutanda, I., Iqbal, M. A., Inafuku, M., Hashimoto, F., et al. (2018). Evaluation of isoprene emission rates of tropical trees by an iterative optimization procedure for G-93 parameters. *Atmos. Environ.* 192, 209–217. doi:10.1016/j.atmosenv.2018.08.059
- Hong, X., Liu, C., Zhang, C., Tian, Y., Wu, H., Yin, H., et al. (2023). Vast ecosystem disturbance in a warming climate may jeopardize our climate goal of reducing CO₂: a case study for megafires in the Australian ‘black summer’. *Sci. Total Environ.* 866, 161387. doi:10.1016/j.scitotenv.2023.161387
- IPCC (2018). “Global Warming of 1.5°C. An IPCC special report on the impacts of global warming of 1.5°C above pre-industrial levels and related global greenhouse gas emission pathways,” in *The context of strengthening the global response to the threat of climate change, sustainable development, and efforts to eradicate poverty*. Eds V. Masson-Delmotte, P. Zhai, H.-O. Pörtner, D. Roberts, J. Skea, P. R. Shukla, and et al. (Switzerland: IPCC).
- Jagadish, S. V. K., Way, D. A., and Sharkey, T. D. (2021). Plant heat stress: concepts directing future research. *Plant Cell Environ.* 44, 1992–2005. doi:10.1111/pce.14050
- Kuhn, U., Rottenberger, S., Biesenthal, T., Wolf, A., Schebeske, G., Ciccioli, P., et al. (2004). Strong correlation between isoprene emission and gross photosynthetic capacity during leaf phenology of the tropical tree species *Hymenaea courbaril* with fundamental changes in volatile organic compounds emission composition during early leaf development. *Plant Cell Environ.* 27, 1469–1485. doi:10.1111/j.1365-3040.2004.01252.x
- Lantz, A. T., Allman, J., Weraduwa, S. M., and Sharkey, T. D. (2019a). Isoprene: new insights into the control of emission and mediation of stress tolerance by gene expression. *Plant Cell Environ.* 42, 2808–2826. doi:10.1111/pce.13629
- Lantz, A. T., Solomon, C., Gog, L., McClain, A. M., Weraduwa, S. M., Cruz, J. A., et al. (2019b). Isoprene suppression by CO₂ is not due to triose phosphate utilization (TPU) limitation. *Front. For. Glob. B.* 2, 8. doi:10.3389/ffgc.2019.00008
- Li, S., Li, X., Wei, Z., and Liu, F. (2020). ABA-mediated modulation of elevated CO₂ on stomatal response to drought. *Curr. Opin. Plant Biol.* 56, 174–180. doi:10.1016/j.pbi.2019.12.002
- Li, Z., and Sharkey, T. D. (2013). Metabolic profiling of the methylerythritol phosphate pathway reveals the source of post-illumination isoprene burst from leaves. *Plant Cell Environ.* 36, 429–437. doi:10.1111/j.1365-3040.2012.02584.x
- Loreto, F., and Schnitzler, J. P. (2010). Abiotic stresses and induced BVOCs. *Trends Plant Sci.* 15, 154–166. doi:10.1016/j.tplants.2009.12.006
- Loreto, F., and Sharkey, T. D. (1990). A gas-exchange study of photosynthesis and isoprene emission in *Quercus-rubra* L. *Planta* 182, 523–531. doi:10.1007/bf02341027
- McClain, A. M., and Sharkey, T. D. (2019). Triose phosphate utilization and beyond: from photosynthesis to end product synthesis. *J. Exp. Bot.* 70, 1755–1766. doi:10.1093/jxb/erz058
- Mentel, T. F., Kleist, E., Andres, S., Dal Maso, M., Hohaus, T., Kiendler-Scharr, A., et al. (2013). Secondary aerosol formation from stress-induced biogenic emissions and possible climate feedbacks. *Atmos. Chem. Phys.* 13, 8755–8770. doi:10.5194/acp-13-8755-2013
- Messina, P., Lathiere, J., Sindelarova, K., Vuichard, N., Granier, C., Ghattas, J., et al. (2016). Global biogenic volatile organic compound emissions in the ORCHIDEE and MEGAN models and sensitivity to key parameters. *Atmos. Chem. Phys.* 16, 14169–14202. doi:10.5194/acp-16-14169-2016
- Monson, R. K., and Fall, R. (1989). Isoprene emission from aspen leaves - influence of environment and relation to photosynthesis and photorespiration. *Plant Physiol.* 90, 267–274. doi:10.1104/pp.90.1.267
- Monson, R. K., Jones, R. T., Rosenstiel, T. N., and Schnitzler, J. P. (2013). Why only some plants emit isoprene. *Plant Cell Environ.* 36, 503–516. doi:10.1111/pce.12015
- Monson, R. K., Neice, A. A., Trahan, N. A., Shiach, I., McCorkel, J. T., and Moore, D. J. (2016). Interactions between temperature and intercellular CO₂ concentration in controlling leaf isoprene emission rates. *Plant Cell Environ.* 39, 2404–2413. doi:10.1111/pce.12787
- Monson, R. K., Trahan, N., Rosenstiel, T. N., Veres, P., Moore, D., Wilkinson, M., et al. (2007). Isoprene emission from terrestrial ecosystems in response to global change: minding the gap between models and observations. *Philos. Trans. R. Soc. A-Math. Phys. Eng. Sci.* 365, 1677–1695. doi:10.1098/rsta.2007.2038
- Morfopoulos, C., Sperlich, D., Penuelas, J., Filella, I., Llusia, J., Medlyn, B. E., et al. (2014). A model of plant isoprene emission based on available reducing power captures responses to atmospheric CO₂. *New Phytol.* 203, 125–139. doi:10.1111/nph.12770
- Mu, Z., Llusia, J., Zeng, J., Zhang, Y., Asensio, D., Yang, K., et al. (2022). An overview of the isoprenoid emissions from tropical plant species. *Front. Plant Sci.* 13, 833030. doi:10.3389/fpls.2022.833030
- Mutanda, I., Inafuku, M., Iwasaki, H., Saitoh, S., Fukuta, M., Watanabe, K., et al. (2016). Parameterization of G-93 isoprene emission formula for tropical trees *Casuarina equisetifolia* and *Ficus septica*. *Atmos. Environ.* 141, 287–296. doi:10.1016/j.atmosenv.2016.06.052
- Niinemetts, U., Rasulov, B., and Talts, E. (2021). CO₂-responsiveness of leaf isoprene emission: why do species differ? *Plant Cell Environ.* 44, 3049–3063. doi:10.1111/pce.14131
- Niinemetts, U., and Sun, Z. (2015). How light, temperature, and measurement and growth CO₂ interactively control isoprene emission in *hybrid aspen*. *J. Exp. Bot.* 66, 841–851. doi:10.1093/jxb/eru443
- Niinemetts, Ü., Tenhunen, J. D., Harley, P. C., and Steinbrecher, R. (1999). A model of isoprene emission based on energetic requirements for isoprene synthesis and leaf photosynthetic properties for *Liquidambar* and *Quercus*. *Plant Cell Environ.* 22, 1319–1335. doi:10.1046/j.1365-3040.1999.00505.x
- Oikawa, P. Y., and Lerdau, M. T. (2013). Catabolism of volatile organic compounds influences plant survival. *Trends Plant Sci.* 18, 695–703. doi:10.1016/j.tplants.2013.08.011
- Ouyang, L., Arnold, R. L., Chen, S., Xie, Y., He, S., Liu, X., et al. (2022). Prediction of the suitable distribution of *Eucalyptus grandis* in China and its responses to climate change. *New For* 53, 81–99. doi:10.1007/s11056-021-09845-2
- Peñuelas, J., and Staudt, M. (2010). BVOCs and global change. *Trends Plant Sci.* 15, 133–144. doi:10.1016/j.tplants.2009.12.005
- Piao, S., Tan, K., Nan, H., Ciais, P., Fang, J., Wang, T., et al. (2012). Impacts of climate and CO₂ changes on the vegetation growth and carbon balance of Qinghai-Tibetan grasslands over the past five decades. *Glob. Planet. Change* 98–99, 73–80. doi:10.1016/j.gloplacha.2012.08.009
- Pierce, T., Geron, C., Bender, L., Dennis, R., Tonnesen, G., and Guenther, A. (1998). Influence of increased isoprene emissions on regional ozone modeling. *J. Geophys. Res. Atmos.* 103, 25611–25629. doi:10.1029/98jd01804

- Possell, M., and Hewitt, C. N. (2011). Isoprene emissions from plants are mediated by atmospheric CO₂ concentrations. *Glob. Change Biol.* 17, 1595–1610. doi:10.1111/j.1365-2486.2010.02306.x
- Possell, M., Nicholas Hewitt, C., and Beerling, D. J. (2005). The effects of glacial atmospheric CO₂ concentrations and climate on isoprene emissions by vascular plants. *Glob. Change Biol.* 11, 60–69. doi:10.1111/j.1365-2486.2004.00889.x
- Potosnak, M. J., LeSturgeon, L., and Nunez, O. (2014). Increasing leaf temperature reduces the suppression of isoprene emission by elevated CO₂ concentration. *Sci. Total Environ.* 481, 352–359. doi:10.1016/j.scitotenv.2014.02.065
- Rapparini, F., Baraldi, R., Miglietta, F., and Loreto, F. (2004). Isoprenoid emission in trees of *Quercus pubescens* and *Quercus ilex* with lifetime exposure to naturally high CO₂ environment. *Plant Cell Environ.* 27, 381–391. doi:10.1111/j.1365-3040.2003.01151.x
- Rasulov, B., Huve, K., Valbe, M., Laik, A., and Niinemets, U. (2009). Evidence that light, carbon dioxide, and oxygen dependencies of leaf isoprene emission are driven by energy status in *hybrid aspen*. *Plant Physiol.* 151, 448–460. doi:10.1104/pp.109.141978
- Rasulov, B., Talts, E., Bichele, I., and Niinemets, U. (2018). Evidence that isoprene emission is not limited by cytosolic metabolites. Exogenous malate does not invert the reverse sensitivity of isoprene emission to high [CO₂]. *Plant Physiol.* 176, 1573–1586. doi:10.1104/pp.17.01463
- Rasulov, B., Talts, E., and Niinemets, U. (2016). Spectacular oscillations in plant isoprene emission under transient conditions explain the enigmatic CO₂ response. *Plant Physiol.* 172, 2275–2285. doi:10.1104/pp.16.01002
- Rosenstiel, T. N., Potosnak, M. J., Griffin, K. L., Fall, R., and Monson, R. K. (2003). Increased CO₂ uncouples growth from isoprene emission in an agriforest ecosystem. *Nature* 421, 256–259. doi:10.1038/nature01312
- Sahu, A., Mostofa, M. G., Weraduwege, S. M., and Sharkey, T. D. (2023). Hydroxymethylbutenyl diphosphate accumulation reveals MEP pathway regulation for high CO₂-induced suppression of isoprene emission. *Proc. Natl. Acad. Sci. U.S.A.* 120, e2309536120. doi:10.1073/pnas.2309536120
- Sharkey, T. D., and Monson, R. K. (2014). The future of isoprene emission from leaves, canopies and landscapes. *Plant Cell Environ.* 37, 1727–1740. doi:10.1111/pce.12289
- Sharkey, T. D., Preiser, A. L., Weraduwege, S. M., and Gog, L. (2020). Source of ¹²C in Calvin-Benson cycle intermediates and isoprene emitted from plant leaves fed with ¹³CO₂. *Biochem. J.* 477, 3237–3252. doi:10.1042/bcj20200480
- Sharkey, T. D., Singsaas, E. L., Lerdau, M. T., and Geron, C. D. (1999). Weather effects on isoprene emission capacity and applications in emissions algorithms. *Ecol. Appl.* 9, 1132–1137. doi:10.1890/1051-0761(1999)009[1132:Weoiec]2.0.Co;2
- Sindelarova, K., Granier, C., Bouarar, I., Guenther, A., Tilmes, S., Stavrou, T., et al. (2014). Global data set of biogenic VOC emissions calculated by the MEGAN model over the last 30 years. *Atmos. Chem. Phys.* 14, 9317–9341. doi:10.5194/acp-14-9317-2014
- Sun, Z., Niinemets, U., Hueve, K., Noe, S. M., Rasulov, B., Copolovici, L., et al. (2012). Enhanced isoprene emission capacity and altered light responsiveness in aspen grown under elevated atmospheric CO₂ concentration. *Glob. Change Biol.* 18, 3423–3440. doi:10.1111/j.1365-2486.2012.02789.x
- Van der Velde, I. R., van der Werf, G. R., Houweling, S., Maasakkers, J. D., Borsdorff, T., Landgraf, J., et al. (2021). Vast CO₂ release from Australian fires in 2019–2020 constrained by satellite. *Nature* 597, 366–369. doi:10.1038/s41586-021-03712-y
- Wang, C., Lu, W., Lin, Y., and Luo, J. (2013). Floristic geography of Eucalyptus and ecological assessment within this distribution. *Eucalypt Sci. and Technol.* 30, 44–51. doi:10.13987/j.cnki.askj.2013.04.010
- Wang, Q., Wu, Y., Wu, W., Lyu, L., and Li, W. (2024). A review of changes at the phenotypic, physiological, biochemical, and molecular levels of plants due to high temperatures. *Planta* 259, 57. doi:10.1007/s00425-023-04320-y
- Wilkinson, M. J., Monson, R. K., Trahan, N., Lee, S., Brown, E., Jackson, R. B., et al. (2009). Leaf isoprene emission rate as a function of atmospheric CO₂ concentration. *Glob. Change Biol.* 15, 1189–1200. doi:10.1111/j.1365-2486.2008.01803.x
- Yang, W., Cao, J., Wu, Y., Kong, F., and Li, L. (2021). Review on plant terpenoid emissions worldwide and in China. *Sci. Total Environ.* 787, 147454. doi:10.1016/j.scitotenv.2021.147454
- Zeng, J., Song, W., Zhang, Y., Mu, Z., Pang, W., Zhang, H., et al. (2022a). Emissions of isoprenoids from dominant tree species in subtropical China. *Front. For. Glob. Change* 5, 1089676. doi:10.3389/ffgc.2022.1089676
- Zeng, J., Zhang, Y., Mu, Z., Pang, W., Zhang, H., Wu, Z., et al. (2023). Temperature and light dependency of isoprene and monoterpene emissions from tropical and subtropical trees: field observations in south China. *Appl. Geochem.* 155, 105727. doi:10.1016/j.apgeochem.2023.105727
- Zeng, J., Zhang, Y., Pang, W., Ran, H., Guo, H., Song, W., et al. (2024). Optimizing in-situ measurement of representative BVOC emission factors considering intraspecific variability. *Geophys. Res. Lett.* 51, e2024GL108870. doi:10.1029/2024gl108870
- Zeng, J., Zhang, Y., Zhang, H., Song, W., Wu, Z., and Wang, X. (2022b). Design and characterization of a semi-open dynamic chamber for measuring biogenic volatile organic compound (BVOC) emissions from plants. *Atmos. Meas. Tech.* 15, 79–93. doi:10.5194/amt-15-79-2022
- Zhang, Y., and Wang, X. (2021). Geographical spatial distribution and productivity dynamic change of eucalyptus plantations in China. *Sci. Rep.* 11, 19764. doi:10.1038/s41598-021-97089-7